Cell Type–Specific Roles of CD38 in the Interactions of Isoniazid with NAD⁺ in the Liver

Junjie Zhu, Jie Lu, Hung-Chun Tung, Ke Liu, Jianhua Li, Denis M. Grant, Wen Xie, and Xiaochao Ma

Center for Pharmacogenetics, Department of Pharmaceutical Sciences, School of Pharmacy, University of Pittsburgh, Pittsburgh, Pennsylvania (J.Z., J.L., H.-C.T., K.L., J.L., W.X., X.M.) and Department of Pharmacology and Toxicology, Faculty of Medicine, University of Toronto, Toronto, Ontario, Canada (D.M.G.)

ABSTRACT

NAD⁺ is a critical molecule that is involved in multiple cellular functions. CD38 is a multifunctional enzyme with NAD⁺ nucleosidase activity. Our previous work revealed the CD38-dependent interactions of isoniazid (INH), an antituberculosis drug, with NAD⁺ to form INH-NAD adduct. In the current work, our metabolomic analysis discovered a novel NAD⁺ adduct with acetylisoniazid (AcINH), a primary INH metabolite mediated by *N*-acetyltransferase (NAT), and we named it AcINH-NAD. Using Nat1/2(−/−) and Cd38(−/−) mice, we determined that AcINH-NAD formation is dependent on both NAT and CD38. Because NAT is expressed in hepatocytes (HP), whereas CD38 is expressed in Kupffer cells (KC) and hepatic stellate cells (HSC), we explored cell type–specific roles of CD38 in the formation of AcINH-NAD as well as INH-NAD. We found that both INH-NAD and AcINH-NAD were produced in the incubation of INH or AcINH with KC and HSC but not in HP. These data suggest that hepatic nonparenchymal cells, such as KC and HSC, are the major cell types responsible for the CD38-dependent interactions of INH with NAD⁺ in the liver.

SIGNIFICANCE STATEMENT

The current study identified AcINH-NAD as a novel metabolite of INH in the liver. Our work also revealed the essential roles of nonparenchymal cells, including Kupffer cells and hepatic stellate cells, in the CD38-dependent interactions of NAD⁺ with INH, leading to the formation of both INH-NAD and AcINH-NAD in the liver. These data can be used to guide the future studies on the mechanisms of INH and NAD⁺ interactions and their contributions to INH-induced liver injury.

Introduction

Tuberculosis is a major public health problem worldwide and has caused around 1.3 million deaths in 2017 (World Health Organization, 2018). Isoniazid (INH, isonicotinohydrazide), discovered in 1952, remains the first-line drug for tuberculosis prophylaxis and therapy. However, INH treatment is accompanied with potential adverse events, including hepatotoxicity. Approximately 10%–20% of INH-treated patients have a transient elevation of plasma aminotransferases, and about 1% of patients encounter liver injury and even fulminant liver failure (Scharer and Smith, 1969; Garibaldi et al., 1972; Nolan et al., 1999). Although the underlying mechanisms of INH-induced liver injury have not yet been defined, INH metabolism is thought to be related to INH hepatotoxicity (Nelson et al., 1976; Timbrell et al., 1980; Sarich et al., 1996; Boelsterli and Lee, 2014; Wang et al., 2016).

The primary metabolic pathway of INH metabolism is acetylation of the hydrazide group catalyzed by *N*-acetyltransferase (NAT) 2, producing acetylisoniazid (AcINH) (Peters et al., 1965; Ellard et al., 1972). INH can also be hydrolyzed by amidases to produce isonicotinic acid and hydrazine (Hz). In addition, AcINH can be hydrolyzed by amidases to produce isonicotinic acid and acetylhydrazine (AcHz), whereas Hz can be further acetylated by NAT2 to produce AcHz and diacetylhydrazine. Hz and AcHz have been proposed as substrates of CYP2E1, which may lead to the production of reactive metabolites (Delaney and Timbrell, 1995; Sarich et al., 1999; Yue et al., 2004). However, no convincing data are available to support the role of CYP2E1 in Hz, AcHz, or INH metabolism (Cheng et al., 2013). Moreover, no convincing data are available to prove the association of these classic pathways of INH metabolism with INH hepatotoxicity in vivo.

Interactions of INH with endobiotics in the liver provide novel insights into the underlying mechanisms of INH hepatotoxicity (Li et al., 2016). INH directly reacts with various ketones and aldehydes like pyruvic acid and pyridoxal to form INH-pyruvic acid adduct and INH-pyridoxal adduct, respectively (Zamboni and Defranceschi, 1954; Wiegand, 1956; Li et al., 2011, 2016). INH can also conjugate with fatty acids and lead to accumulation of acylcarnitines in mouse

TABLE 1
Primers for qPCR analysis

| Gene	Orientation	Sequence (5′–3′)
Albumin	Forward	TGCTTTTTCCAGGGGTGTGTT
	Reverse	TTACTTCCTGCACTAATTTGGCA
F4/80	Forward	GCTGTGAGATTGTGGGAAGCA
	Reverse	ATGGCCAAGGCAAGACATAC
Clec4f	Forward	GAGGCCGAGCTGAACAGAG
	Reverse	TGTGAAGCCACCACAAAAAGAG
Desmin	Forward	GCCACCTACCGGAAGCTACT
	Reverse	GCAGAGAAGGTCTGGATAGGAA
α-Sma	Forward	AAACAGGAATACGACGAAG
	Reverse	CAGGAATGATTTGGAAAGGA
Cyp2e1	Forward	CAAGTCTTTAACCAAGTTGGCAAA
	Reverse	CCACGATGCGCCTCTGA
Nat1	Forward	GATTTACAGGACATTTTTGACCACATAGTA
	Reverse	CACCTGTACTAGAAGGTGGACCATTT
Cd38	Forward	TTGCAAGGGTTCTTGGAAAC
	Reverse	CGCTGCCTCATCTACACTCA
Cyclophilin	Forward	TGGAGAGCACCAAGACAGACA
	Reverse	GCCCGTAGTGCTTCAGCTT

liver (Li et al., 2016). Additionally, INH causes protoporphyrin IX accumulation in the liver through the induction of δ-aminolevulinate synthase 1 and downregulation of ferrochelatase (Sachar et al., 2016). Furthermore, INH can react with NAD⁺ to form INH-NAD adduct

(1-(((2R,3R,4S,5R)-5-(((((((((2R,3S,4R,5R)-5-(6-amino-9H-purin-9-yl)-3,4-dihydroxytetrahydrofuran-2-yl)methoxy)(hydroxy)phosphoryl) oxy)(hydroxy)phosphoryl)oxy)methyl)-3,4-dihydroxytetrahydrofuran-2-yl)-4-(hydrazinecarbonyl)pyridin-1-ium) as catalyzed by CD38, a multifunctional enzyme with NAD⁺ nucleosidase activity (Zatman et al., 1954; Li et al., 2016; Chini et al., 2018).

NAD⁺ is involved in multiple cellular functions, including redox reactions, DNA repair, cell cycle regulation, and calcium signaling (Malavasi et al., 2008; Lee, 2012; Stein and Imai, 2012; Fouquerel and Sobol, 2014; Imai and Guarente, 2014; Chini et al., 2018). Interactions between NAD⁺ and INH may disrupt NAD⁺ homeostasis and in turn lead to cellular dysfunctions. Hence, a comprehensive study on the interactions between INH and NAD⁺ is needed. Using a metabolomic approach, the current work revealed a novel NAD⁺ adduct with INH metabolite AcINH in the liver—namely, AcINH-NAD (4-(2-acetylhydrazinecarbonyl)-1-(((2R,3R,4S,5R)-5-(((((((((2R,3S,4R,5R)-5-(6-amino-9H-purin-9-yl)-3,4-dihydroxytetrahydrofuran-2-yl)methoxy)(hydroxy) phosphoryl)oxy)(hydroxy)phosphoryl)oxy)methyl)-3,4-dihydroxytetrahydrofuran-2-yl)pyridin-1-ium). Additionally, genetically engineered mouse models, including Nat1/2(−/−) and Cd38(−/−) mice, were used to determine the roles of NAT and CD38 in the formation of INH-NAD and AcINH-NAD, respectively. Because NAT is expressed in hepatocytes (HP), whereas CD38 is expressed in Kupffer cells (KC) and hepatic stellate cells (HSC) (Oesch and Steinberg, 1987; March et al.,
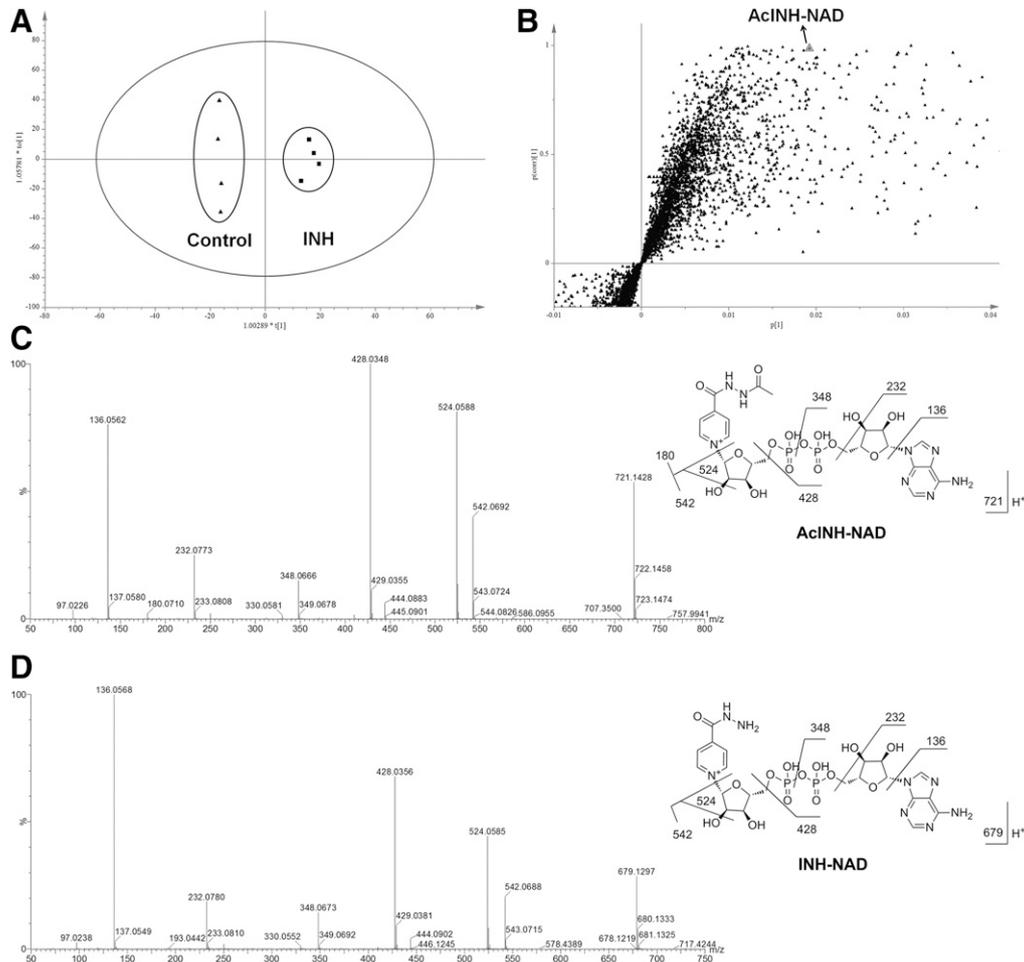
Fig. 1. Identification of AcINH-NAD by a metabolomic analysis of mouse liver. WT mice were treated with vehicle (control) or INH (73 mg/kg, by mouth) for 1 hour. Liver samples were collected and analyzed by UPLC-QTOFMS. (A) Separation of liver samples from control and INH groups in an OPLS-DA score plot. (B) A loading S-plot generated by OPLS-DA analysis. (C) MS/MS spectrum of AcINH-NAD. (D) MS/MS spectrum of INH-NAD. The structures of AcINH-NAD and INH-NAD with MS/MS fragmentation patterns are inlaid in the spectra.

A

B

C

D
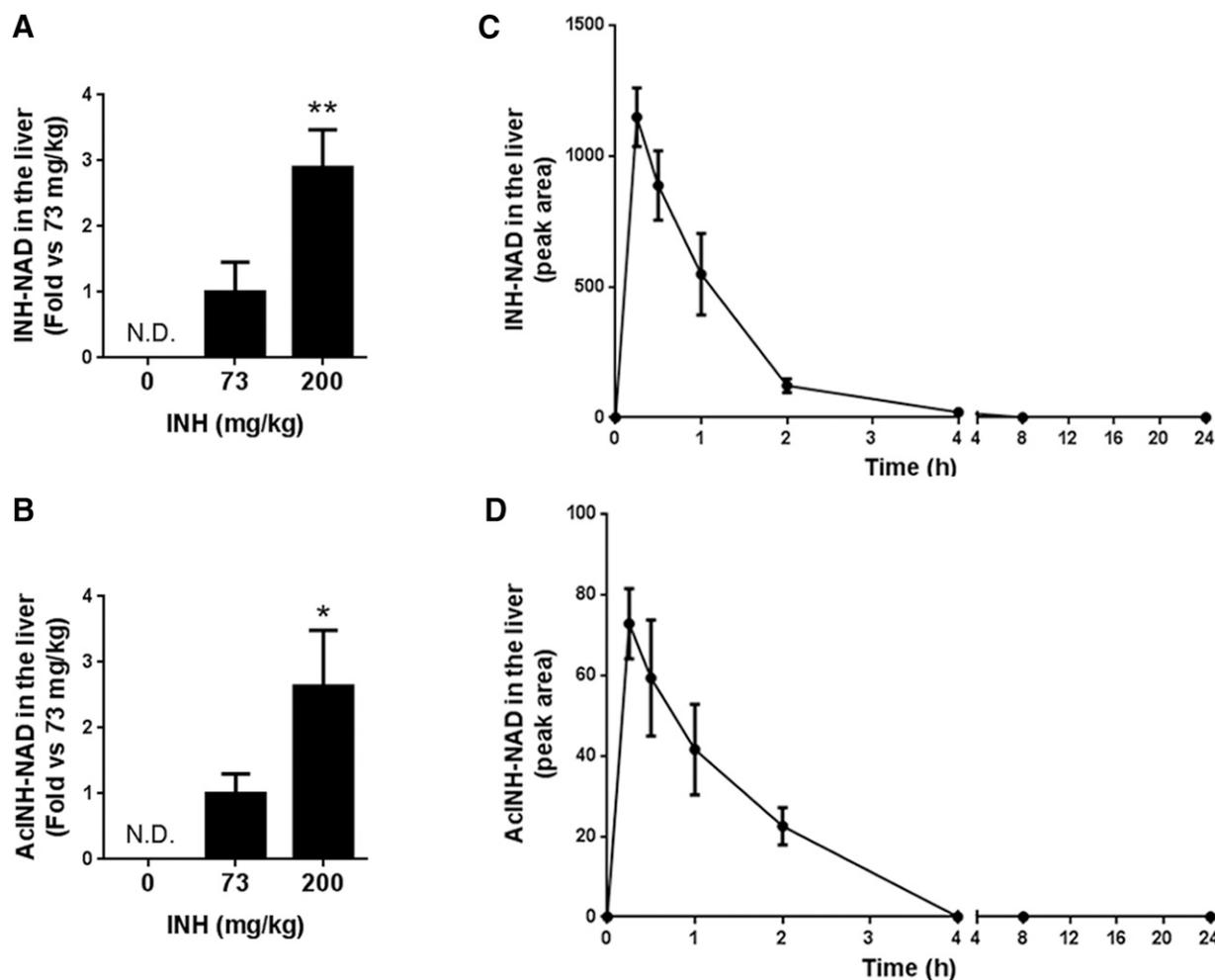
Fig. 2. Dose response and pharmacokinetics of INH-NAD and AcINH-NAD in the liver. (A and B) Relative abundance of INH-NAD (A) and AcINH-NAD (B) in the liver of mice treated with different doses of INH. WT mice were orally treated with vehicle (control) or INH at 73 or 200 mg/kg. Livers were collected at 15 minutes after treatment. The abundance of INH-NAD and AcINH-NAD in the 73-mg/kg group was set as 1, respectively. N.D., not detected. (C and D) Pharmacokinetics of INH-NAD (C) and AcINH-NAD (D) in the liver of WT mice treated with INH (73 mg/kg, by mouth). Livers were harvested at 0, 0.25, 0.5, 1, 2, 4, 8, and 24 hours postdose. INH-NAD and AcINH-NAD were extracted from the liver and analyzed by UPLC-QTOFMS. The data are expressed as means ± S.D. (n = 4). *P < 0.05; **P < 0.01 vs. 73-mg/kg group.

2007), we further explored the cell type–specific roles of CD38 in the formation of INH-NAD and AcINH-NAD by using primary mouse liver cells, including HP, KC, and HSC.

Materials and Methods

Chemicals and Reagents. INH, NAD$^+$, CD38 from porcine brain, and ammonium acetate (AcONH$_4$) were purchased from Sigma-Aldrich (St. Louis, MO). AcINH was purchased from Toronto Research Chemical (Toronto, ON, Canada). Nicotinamide-2,4,5,6-d$_4$ was purchased from CDN Isotopes (Pointe-Claire, QC, Canada). All solvents for ultra-performance liquid chromatography and quadrupole time-of-flight mass spectrometry (UPLC-QTOFMS) analysis were of the highest grade commercially available.

Animals and Treatments. Nat1/2(−/−) mice were generated and provided by Dr. Denis M. Grant's laboratory (Sugamori et al., 2003). Cd38(−/−) mice were purchased from the Jackson Laboratory. Wild-type (WT), Nat1/2(−/−), and Cd38(−/−) mice (male, 8–12 weeks old, C57BL/6 background) were treated with vehicle (water) or INH (73 mg/kg, by mouth). At 1 hour later, mouse livers were harvested and stored at −80°C until further analysis. For the dose-dependent effects of INH on the formation of INH-NAD and AcINH-NAD in the liver, WT mice were treated with INH (73 or 200 mg/kg, by mouth), and the livers were collected 15 minutes postdose. For the pharmacokinetic analysis of INH-NAD and AcINH-NAD, WT mice were treated with INH (73 mg/kg, by mouth), and mouse sera and livers were harvested at 0, 0.25, 0.5, 1, 2, 4, 8, and 24 hours

postdose. All animal studies were approved by the Institutional Animal Care and Use Committee of the University of Pittsburgh.

Sample Preparation for Metabolite Analysis. The extraction of metabolites from mouse livers was performed according to a previous report, with a minor modification (Zhu et al., 2018). In brief, 100 mg of liver sample was homogenized in 600 μl of water containing nicotinamide-2,4,5,6-d$_4$ as an internal standard, and then 1.2 ml of acetonitrile/methanol (1:1, v/v) was added to the resulting suspension. The mixture was mixed on a vortex mixer for 2 minutes, followed by centrifugation at 15,000 rpm for 10 minutes. A 2-μl aliquot of the supernatant was injected into the UPLC-QTOFMS system for metabolite analysis.

Formation of AcINH-NAD in the Incubation with AcINH and CD38. Incubations were carried out in 1× PBS (pH = 7.4) containing porcine CD38 (1.0 mg/ml), 2 mM NAD$^+$, and 200 μM AcINH in a final volume of 100 μl. The groups in the absence of CD38 or NAD$^+$ or AcINH were used as controls. After 2 hours of incubation at 37°C, the reactions were terminated by adding 100 μl of acetonitrile. The mixture was then mixed on a vortex mixer and centrifuged at 15,000 rpm for 10 minutes. A 5-μl aliquot of the supernatant was injected into the UPLC-QTOFMS system for AcINH-NAD analysis.

Isolation and Culture of Primary Mouse Liver Cells. Livers from WT mice (male, 8–12 weeks old) were perfused with calcium and magnesium-free Hanks' balanced salt solution (Hyclone, Logan, UT) and digested with Liberase TM (Roche, Mannheim, Germany). The resulting cell suspension was filtered through a 100-μm cell strainer and further centrifuged at 500 rpm for 3 minutes at 4°C. The supernatants were rich in nonparenchymal cells (NPC). The pellet containing

HP was washed twice with cold Williams' E medium (Sigma-Aldrich), and then HP were seeded onto six-well plates precoated with type 1 collagen (Discovery Labware, Bedford, MA) in Williams' E medium containing 5% FBS. After the attachment of HP, the culture medium was changed to HepatoZYME-SFM (Thermo Fisher Scientific, Carlsbad, CA), a hepatocyte maintenance medium. HSC were isolated from the NPC fraction by Nycodenz (Accurate Chemical, Westbury, NY) density gradient centrifugation as previously described (Mederacke et al., 2015). Isolated HSC were seeded onto six-well plates with Dulbecco's modified Eagle's medium (Sigma-Aldrich) containing 10% FBS, and morphology was checked under light microscopy. KC were isolated from the NPC fraction using Percoll (Sigma-Aldrich) density gradient centrifugation and purified by selective adherence following prior reports (Smedsrød and Pertoft, 1985; Cabral et al., 2018). KC were cultured with RPMI 1640 medium (Hyclone) containing 10% FBS. All the primary cells were incubated at 37°C under a 5% CO_2-humidified atmosphere. HP, KC, and HSC were verified by quantitative real-time polymerase chain reaction (qPCR) analysis of cell type–specific genes (Table 1).

qPCR Analysis. Total RNA was extracted from cells using TRIzol reagent, and cDNA was prepared using random hexamer primers and Moloney Murine Leukemia Virus Reverse Transcriptase (Thermo Fisher Scientific). qPCR was performed using the QuantStudio 6 Flex System (Applied Biosystems, Foster City, CA). The qPCR primers of target genes are listed in Table 1. The expression level of each target gene was normalized against cyclophilin.

Formation of INH-NAD and AcINH-NAD in Primary Mouse Liver Cells. HP, KC, and HSC were incubated with 1 mM NAD⁺ and different concentrations of INH (100, 500, and 1000 μM) or AcINH (50, 250, and 500 μM) in corresponding culture medium. At 4 hours later, 100 μl of medium was collected and mixed with 100 μl of methanol/acetonitrile (1:1, v/v) to precipitate proteins. The postcentrifugation (15,000 rpm for 10 minutes) supernatants were injected into UPLC-QTOFMS for the analyses of INH-NAD and AcINH-NAD. Meanwhile, cells were harvested after washing twice with 1× PBS (pH 7.4). The suspension mixture containing cells was sonicated and centrifuged to give supernatants, which were dried and reconstituted in 100 μl of water/acetonitrile (1:1, v/v) for UPLC-QTOFMS analysis. Cellular proteins were extracted by radioimmunoprecipitation assay buffer (Sigma-Aldrich), and total protein concentrations were measured by Pierce BCA protein assay kit (Thermo Fisher Scientific). The abundance of INH-NAD and AcINH-NAD was normalized to cellular protein concentrations.

UPLC-QTOFMS Analysis. The analyses were performed on an Acquity UPLC Ethylene Bridged Hybrid Amide column (2.1 × 150 mm, 1.7 μm) coupled with a SYNAPT G2-S mass spectrometer (Waters Corporation, Milford, MA). The column temperature was set at 50°C. The mobile phases for the separation were A (10 mM $AcONH_4$, 5% acetonitrile in water) and B (10 mM $AcONH_4$, 5% water in acetonitrile). The elution gradient was set as follows: 0.0–1.0 minute, 15% A; 1.0–7.0 minutes, 15%–60% A; 7.0–10.0 minutes, 60% A; 10.0–10.5 minutes, 60%–1% A; 10.5–13.0 minutes, 1% A; 13.0–13.5 minutes, 1%–15% A; 13.5–15.0 minutes, 15% A. The QTOFMS system was operated in a positive high-resolution mode with electrospray ionization. The mass parameters were set as previously reported (Liu et al., 2017; Zhu et al., 2018). Collision energy ramping from 10 to 45 eV was used for structural elucidation of INH metabolites.

Data Analysis. Multivariate data analyses of the liver samples were performed similarly as previously reported (Liu et al., 2017; Zhu et al., 2018). In brief, the mass data acquired by MassLynx 4.1 were exported into SIMCA-P software (version 13; Umetrics, Kinnelon, NJ), and orthogonal partial least-squares discriminant analysis (OPLS-DA) was further conducted to maximize the class discrimination. An S-plot was generated and used for screening of novel metabolites. Structures of metabolites were elucidated based on accurate mass measurement (mass errors less than 10 ppm) and tandem mass spectrometry (MS/MS) fragmentation analysis.

Statistical Analysis. Data are expressed as means or means ± S.D. Statistical analyses were performed with a two-tailed Student's *t* test (for two groups) or one-way ANOVA (for multiple groups), and a *P* value <0.05 was considered as statistically significant.

Results

Identification of AcINH-NAD in Mouse Liver. A metabolomic study was conducted for the livers from WT mice treated with vehicle (control) or INH. The control and INH groups were well separated to the
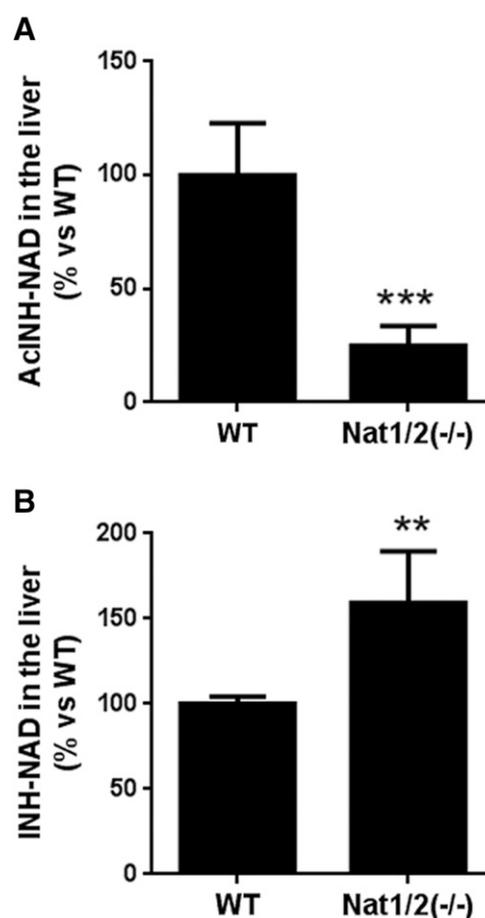
Fig. 3. Role of NAT in AcINH-NAD and INH-NAD formation in the liver of WT and Nat1/2(−/−) mice treated with INH. At 1 hour after INH treatment (73 mg/kg, by mouth), liver samples were collected and analyzed by UPLC-QTOFMS. (A) Relative abundance of AcINH-NAD in the liver of WT and Nat1/2(−/−) mice. (B) Relative abundance of INH-NAD in the liver of WT and Nat1/2(−/−) mice. The abundances of AcINH-NAD and INH-NAD in the liver of WT mice were set as 100%. Data are expressed as means ± S.D. (n = 4). **P < 0.01; ***P < 0.001.

corresponding clusters by OPLS-DA (Fig. 1A). A novel metabolite, named AcINH-NAD herein, ranked as one of the top ions in the S-plot (Fig. 1B). AcINH-NAD was eluted at 5.30 minutes. AcINH-NAD has a protonated molecular ion [M + H] at mass-to-charge ratio (*m/z*) = 721.1428, and the MS/MS fragmentation ions were at *m/z* 542, 524, 428, 348, 232, 180, and 136 (Fig. 1C). The fragmentation ion at *m/z* = 180 indicates the structure of AcINH. By further comparing with the MS/MS of INH-NAD (Fig. 1D), we elucidated the structure of AcINH-NAD, in which the nicotinamide group of NAD⁺ was replaced by AcINH (Fig. 1D).

Dose- and Time-Dependent Formation of INH-NAD and AcINH-NAD in Mouse Liver. The formation of INH-NAD and AcINH-NAD is dose-dependent. INH-NAD and AcINH-NAD are undetectable in the vehicle group. In the group with a high dose of INH (200 mg/kg), the abundance of INH-NAD and AcINH-NAD is significantly higher than that in the lower-dose group (73 mg/kg) (Fig. 2, A and B). We also investigated the pharmacokinetics of INH-NAD and AcINH-NAD in the liver. After INH administration, both INH-NAD and AcINH-NAD were quickly formed in the liver, reached the highest levels at 15 minutes, and then decreased to undetectable levels after 4 hours (Fig. 2, C and D), which is consistent with the pharmacokinetics of hepatic INH and AcINH (Wang et al., 2017). INH-NAD and AcINH-NAD could not be detected in mouse sera after INH
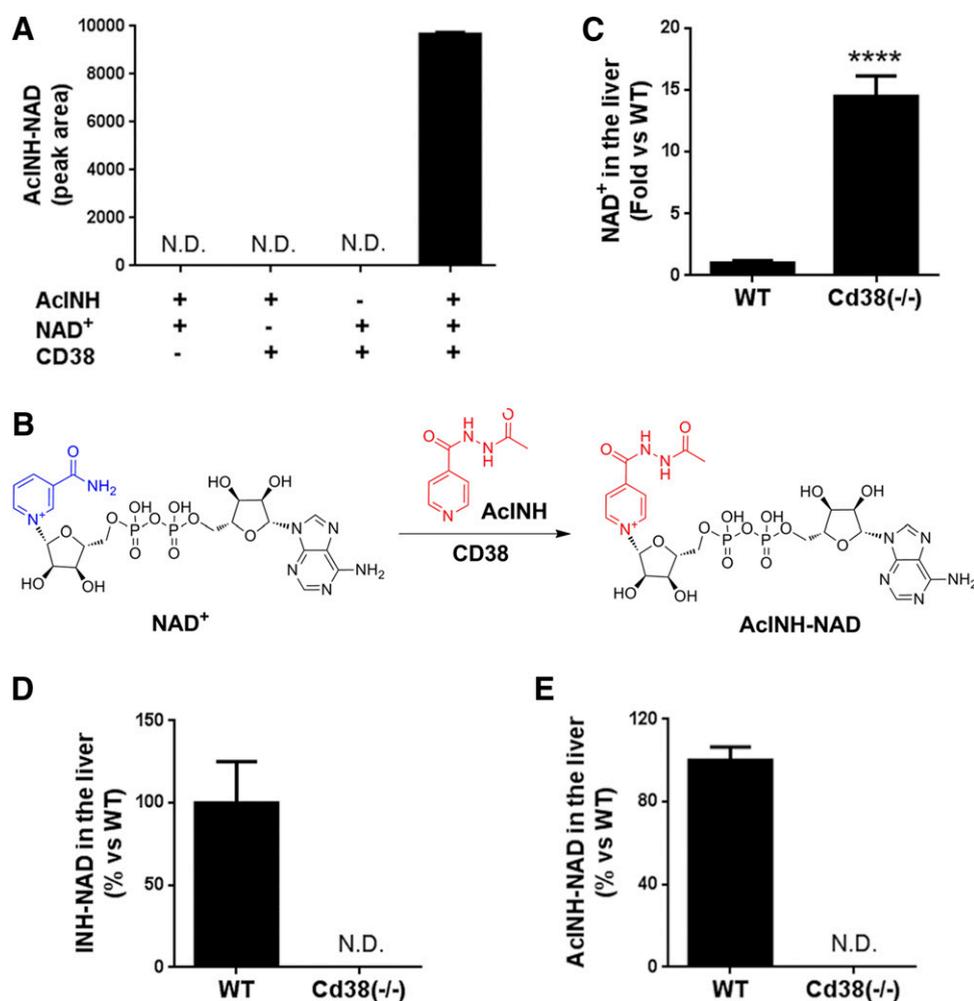
Fig. 4. Role of CD38 in the formation of INH-NAD and AcINH-NAD. (A) Formation of AcINH-NAD in the incubation with AcINH, NAD$^+$, and CD38 ($n = 3$). CD38 (1.0 mg/ml), 2 mM NAD$^+$, and 200 μM AcINH were incubated in a final volume of 100 μl of 1× PBS for 2 hours. (B) Scheme of AcINH-NAD formation. (C) Hepatic NAD$^+$ levels in WT and Cd38($-/-$) mice without INH treatment. The abundance of NAD$^+$ in WT mice was set as 1. (D and E) Formation of INH-NAD (D) and AcINH-NAD (E) in the liver of WT and Cd38($-/-$) mice treated with INH (73 mg/kg, by mouth, $n = 4$). The abundance of INH-NAD and AcINH-NAD in WT mice was set as 100%, respectively. Data are expressed as means ± S.D. N.D., not detected. ****$P < 0.0001$.

treatment. AcINH-NAD seems less abundant than INH-NAD by comparing their peak areas (Fig. 2, C and D), although the differences of their ionization efficiencies cannot be ruled out.

The Role of NAT in the Production of INH-NAD and AcINH-NAD. Nat1/2($-/-$) mice were used to determine the role of NAT in the formation of INH-NAD and AcINH-NAD. Compared with WT mice, hepatic AcINH-NAD was decreased by 75% in Nat1/2($-/-$) mice treated with INH (Fig. 3A), suggesting that NAT plays an important role in AcINH-NAD formation. On the other hand, the abundance of INH-NAD was statistically significantly increased in the liver of Nat1/2($-/-$) mice treated with INH (Fig. 3B), which is because deficiency of NAT slows down INH acetylation, leading to INH accumulation in the liver and therefore increasing the interactions between INH and NAD$^+$. The increase of INH-NAD in the liver of Nat1/2($-/-$) mice is consistent with our previous finding that NAT deficiency increases the interactions of INH with endobiotics in the liver (Wang et al., 2017).

The Role of CD38 in the Production of INH-NAD and AcINH-NAD. To determine the role of CD38 in AcINH-NAD formation, AcINH was incubated with CD38. We found that AcINH-NAD formation was dependent on three components—AcINH, NAD$^+$, and CD38 (Fig. 4A)—which is similar to the CD38-dependent formation of INH-NAD (Li et al., 2016). These data suggest that CD38 hydrolyzes the nicotinamide group from NAD$^+$ and substitutes it with AcINH, leading to the production of AcINH-NAD (Fig. 4B). To further verify the role of CD38 in the formation of AcINH-NAD as well

as INH-NAD, Cd38($-/-$) mice were used. In line with a previous report (Aksoy et al., 2006), NAD$^+$ levels were significantly increased in the liver of Cd38($-/-$) mice (Fig. 4C), suggesting that CD38 is deficient in these mice. After INH treatment, INH-NAD and AcINH-NAD were undetectable in the liver of Cd38($-/-$) mice (Fig. 4, D and E), indicating that the formation of INH-NAD and AcINH-NAD is fully dependent on CD38.

Cell Type–Specific Role of CD38 in the Formation of INH-NAD and AcINH-NAD. We next explored the contribution of HP, KC, and HSC to the formation of INH-NAD and AcINH-NAD. These cells were isolated from mouse liver and characterized by their specific markers, including *F4/80*, C-type lectin domain family 4 member F (*Clec4f*), *Desmin*, and α-smooth muscle actin (α-*Sma*) (Fig. 5, A and B). Based upon the relative expression of these cell type–specific markers, we estimated that the purity of HP is ~100%, and the purity of KC and HSC is ~90%. We also analyzed INH-metabolizing enzymes in these cells, including *Cyp2e1* and *Nat1*. As expected, *Cyp2e1* and *Nat1* are highly expressed in HP but very low in KC and HSC (Fig. 5, C and D). Conversely, *Cd38* is highly expressed in KC and HSC but very low in HP (Fig. 5E), which is consistent with a previous report (March et al., 2007). In agreement with CD38 expression in liver cells (Fig. 5E), Both INH-NAD and AcINH-NAD were produced predominantly in the culture medium of KC and HSC incubated with INH (Fig. 6, A and B) or AcINH (Fig. 6, C and D), but to a much lesser degree in that of HP. These data indicate that KC and HSC are the major cell types responsible for the CD38-mediated formation of INH-NAD and AcINH-NAD in
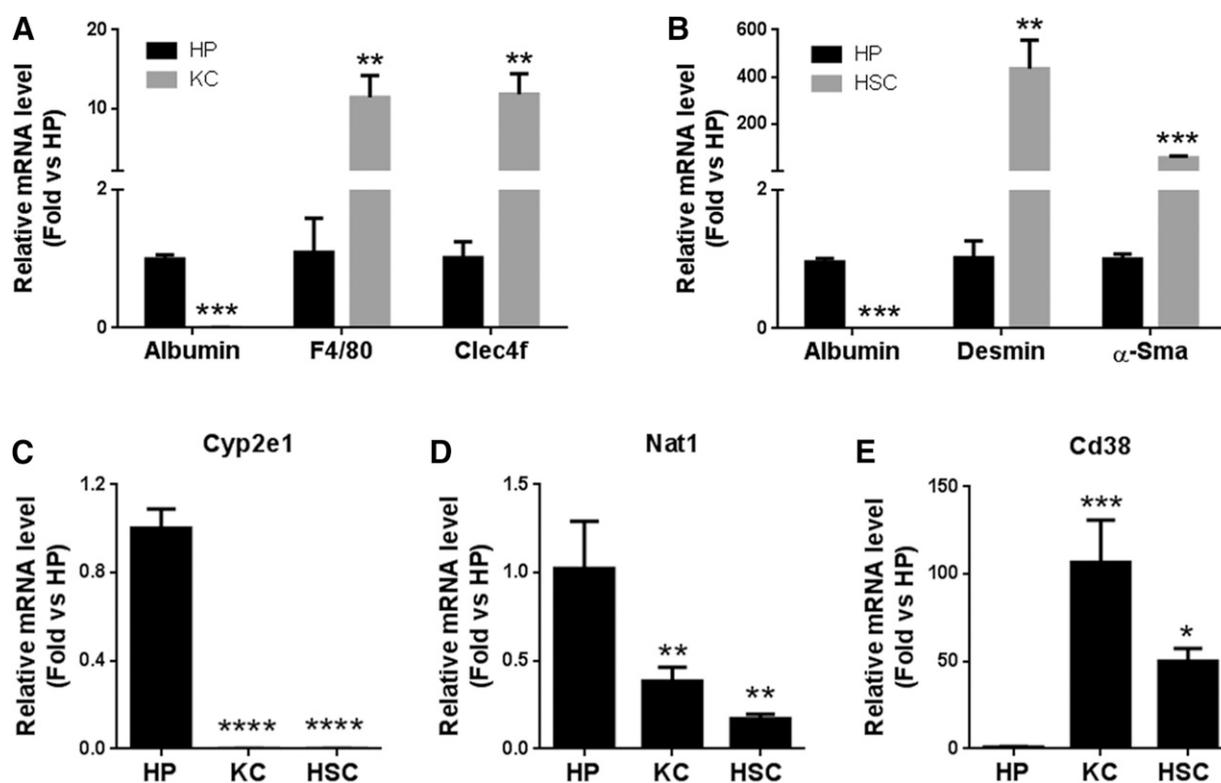
Fig. 5. Expression of INH-metabolizing enzymes in primary mouse liver cells. (A and B) Characterization of HP, KC, and HSC by qPCR: *Albumin* for HP; *F4/80* and *Clec4f* for KC; and *Desmin* and *α-Sma* for HSC. (C–E) mRNA expression of *Cyp2e1* (C), *Nat1* (D), and *Cd38* (E) in HP, KC, and HSC. The data in HP were set as 1. All data are expressed as means ± S.D. ($n = 3$). *$P < 0.05$; **$P < 0.01$; ***$P < 0.001$; ****$P < 0.0001$ vs. HP.

the liver. In addition, intracellular INH-NAD and AcINH-NAD were undetectable, which is attributed to the primary location of CD38 in cell membrane (Malavasi et al., 2008).

Discussion

The current work provided novel insights into the interactions between INH and NAD⁺ in the liver. Using a metabolomic approach, we identified AcINH-NAD as a novel metabolite of INH. Our further studies revealed that AcINH-NAD formation is dependent on both NAT and CD38. Moreover, we determined KC and HSC as the major hepatic cell types contributing to the CD38-dependent formation of AcINH-NAD as well as INH-NAD (Fig. 6E).

The distribution of NAT and CD38 in different cell types determines the production process of INH-NAD and AcINH-NAD in the liver. The liver consists of parenchymal HP and NPC, which account for 60%–70% and 30%–40% of total liver cells, respectively (Alpini et al., 1994; Si-Tayeb et al., 2010). NAT is mainly expressed in HP, whereas CD38 is predominantly expressed in NPC, including KC and HSC (Oesch and Steinberg, 1987; March et al., 2007). KC and HSC locate in the perisinusoidal space (or space of Disse), where INH can be metabolized by CD38 to form INH-NAD. When INH enters HP, it can be metabolized by NAT to produce AcINH, the major metabolite of INH. Next, AcINH is diffused from HP into the perisinusoidal space and thereby exposed to CD38 on KC and HSC, leading to the formation of AcINH-NAD (Fig. 6E).

This is the first study that reveals the contribution of hepatic NPC to INH metabolism. NPC, such as KC and HSC, are capable of metabolizing endobiotics and xenobiotics (Oesch and Steinberg, 1987). KC have been disclosed to uptake and metabolize environmental pollutants (Zhong et al., 1994). HSC have high expression of CYP1B1,

which is responsible for the metabolism of retinoids (Piscaglia et al., 1999; Choudhary et al., 2004; Friedman, 2008). Nevertheless, the current work uncovered the sequential metabolism of INH in HP and NPC, leading to the formation of AcINH-NAD. This process provides an example for the joint activities of multiple cell types to form one metabolite in drug metabolism.

CD38 has NAD⁺ nucleosidase activity that hydrolyzes NAD⁺ to nicotinamide and adenosine diphosphate ribose (Kontani et al., 1993; Aksoy et al., 2006; Chini et al., 2018). In addition, CD38 mediates the replacement action of the nicotinamide group in NAD⁺ by a series of pyridine analogs, including INH (Zatman et al., 1954; Anderson et al., 1959; Li et al., 2016). AcINH has a similar chemical structure as nicotinamide; hence, it is feasible that CD38 catalyzes the interactions of AcINH and NAD⁺, leading to AcINH-NAD formation. Extrapolated from the current work, other pyridine-containing drugs may also interact with NAD⁺ via CD38 to form drug-NAD adducts. NAD⁺ analogs with minor changes in NAD⁺ structure would likely disrupt biologic functions of NAD⁺. Ara-NAD and Carba-NAD, two NAD⁺ analogs with modifications of the ribose group in NAD⁺ structure, are potent CD38 inhibitors (Chini et al., 2018). In addition, introduction of an amino group to the purine moiety of NAD⁺ leads to a more efficient substrate of poly(ADP-ribosyl) transferase than NAD⁺ (Oei et al., 1996). Because of the structural similarities of INH-NAD and AcINH-NAD with NAD⁺, further studies are needed to determine whether INH-NAD and AcINH-NAD disrupt NAD⁺-dependent pathways in the liver.

Cell-cell communications between HP and NPC have been implicated in many physiologic and pathophysiologic processes, including cell growth, migration, and differentiation (Bhatia et al., 1999). KC are the liver resident macrophages, and they are associated with a series of acute and chronic liver diseases through the release of inflammatory mediators and/or reactive oxygen species (Dixon et al., 2013). KC activation also
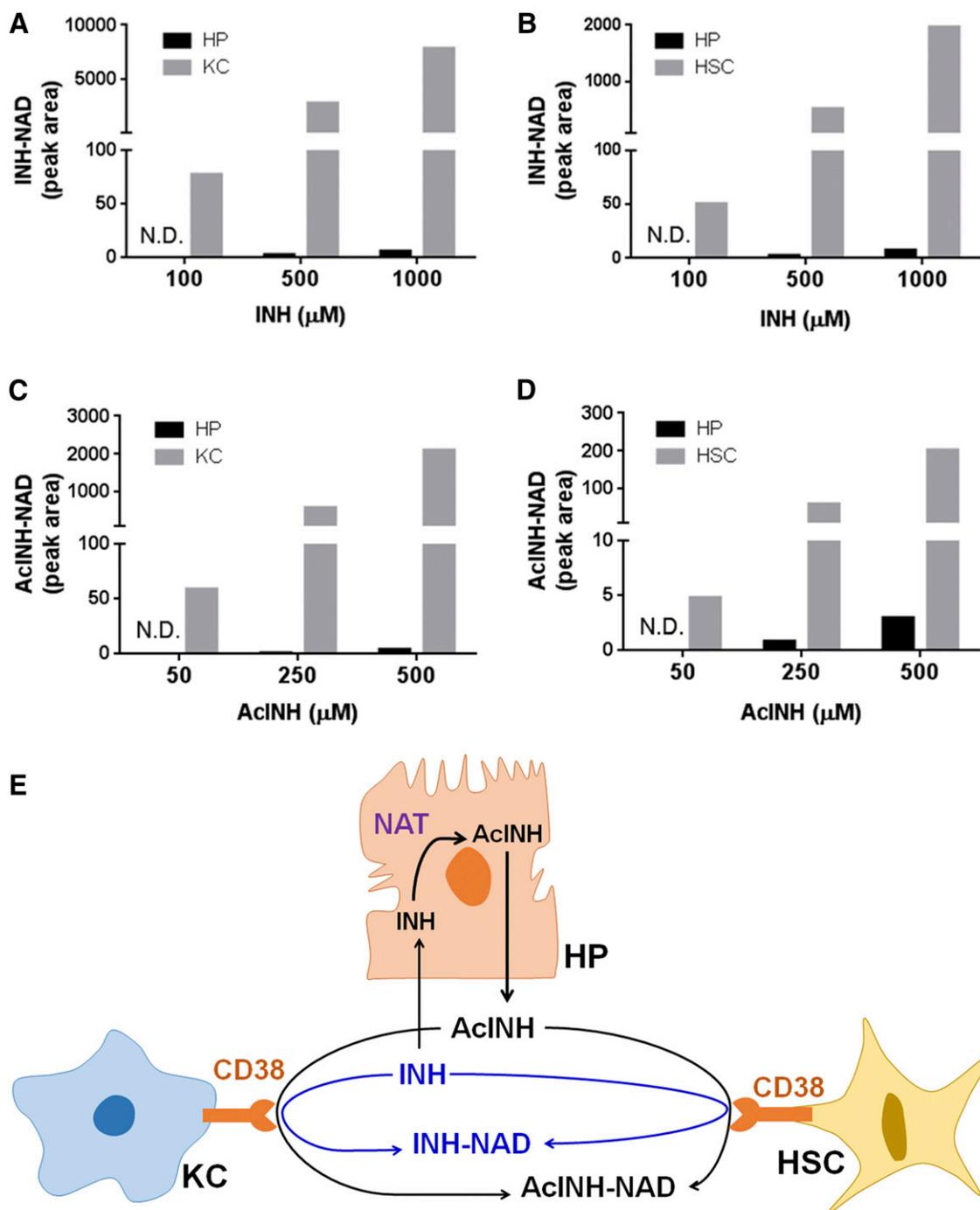
Fig. 6. Formation of INH-NAD and AcINH-NAD in HP, KC, and HSC. HP, KC, and HSC were incubated with 1 mM NAD^+ and different concentrations of INH (100, 500, and 1000 μM) or AcINH (50, 250, and 500 μM) for 4 hours. INH-NAD and AcINH-NAD in the culture medium were measured by UPLC-QTOFMS. (A) Comparison of INH-NAD formation in HP and KC. (B) Comparison of INH-NAD formation in HP and HSC. (C) Comparison of AcINH-NAD formation in HP and KC. (D) Comparison of AcINH-NAD formation in HP and HSC. Data were normalized to protein concentrations and expressed as means ($n = 2$). N.D., not detected. (E) Proposed mechanisms for the formation of INH-NAD and AcINH-NAD in the liver: 1) CD38 in KC and HSC catalyzes the interactions of INH with NAD^+ to form INH-NAD; and 2) acetylation of INH by NAT in HP produces AcINH, which is excreted from HP and further interacts with NAD^+ via CD38 in KC and HSC to form AcINH-NAD.

contributes to drug-induced liver injury (Roberts et al., 2007). HSC are liver fibrogenic cells, which are also involved in hepatic inflammation via the production of cytokines and chemokines (Friedman, 2008). Therefore, further studies are warranted to investigate the effects of INH-NAD and AcINH-NAD on KC and HSC functions and their impact on cell-cell communications between HP and NPC.

In summary, the current work identified AcINH-NAD as a novel metabolite of INH in the liver. Our work also revealed the essential roles of KC and HSC in the CD38-dependent interactions of NAD^+ with INH in the liver. The data from this work can be used to guide the future studies on the mechanisms of INH and NAD^+ interactions and their contributions to INH-induced liver injury.

Authorship Contributions

Participated in research design: Zhu, Ma.

Conducted experiments: Zhu, Lu, Tung, Liu, Li.

References

Aksoy P, White TA, Thompson M, and Chini EN (2006) Regulation of intracellular levels of NAD: a novel role for CD38. *Biochem Biophys Res Commun* **345**:1386–1392.

Alpini G, Phillips JO, Vroman B, and LaRusso NF (1994) Recent advances in the isolation of liver cells. *Hepatology* **20**:494–514.

Anderson BM, Ciotti CJ, and Kaplan NO (1959) Chemical properties of 3-substituted pyridine analogues of diphosphopyridine nucleotide. *J Biol Chem* **234**:1219–1225.

Bhatia SN, Balis UJ, Yarmush ML, and Toner M (1999) Effect of cell-cell interactions in preservation of cellular phenotype: cocultivation of hepatocytes and nonparenchymal cells. *FASEB J* **13**:1883–1900.

Boelsterli UA and Lee KK (2014) Mechanisms of isoniazid-induced idiosyncratic liver injury: emerging role of mitochondrial stress. *J Gastroenterol Hepatol* **29**:678–687.

Cabral F, Miller CM, Kudrna KM, Hass BE, Daubendiek JG, Kellar BM, and Harris EN (2018) Purification of hepatocytes and sinusoidal endothelial cells from mouse liver perfusion. *J Vis Exp* **132**:e56993.

Cheng J, Krausz KW, Li F, Ma X, and Gonzalez FJ (2013) CYP2E1-dependent elevation of serum cholesterol, triglycerides, and hepatic bile acids by isoniazid. *Toxicol Appl Pharmacol* **266**: 245–253.

Chini EN, Chini CCS, Espindola Netto JM, de Oliveira GC, and van Schooten W (2018) The pharmacology of CD38/NADase: an emerging target in cancer and diseases of aging. *Trends Pharmacol Sci* **39**:424–436.

Choudhary D, Jansson I, Stoilov I, Sarfarazi M, and Schenkman JB (2004) Metabolism of retinoids and arachidonic acid by human and mouse cytochrome P450 1b1. *Drug Metab Dispos* **32**: 840–847.

Delaney J and Timbrell JA (1995) Role of cytochrome P450 in hydrazine toxicity in isolated hepatocytes in vitro. *Xenobiotica* **25**:1399–1410.

Dixon LJ, Barnes M, Tang H, Pritchard MT, and Nagy LE (2013) Kupffer cells in the liver. *Compr Physiol* **3**:785–797.

Ellard GA, Gammon PT, and Wallace SM (1972) The determination of isoniazid and its metabolites acetylisoniazid, monoacetylhydrazine, diacetylhydrazine, isonicotinic acid and isonicotinylglycine in serum and urine. *Biochem J* **126**:449–458.

Fouquerel E and Sobol RW (2014) ARTD1 (PARP1) activation and NAD(+) in DNA repair and cell death. *DNA Repair (Amst)* **23**:27–32.

Friedman SL (2008) Hepatic stellate cells: protean, multifunctional, and enigmatic cells of the liver. *Physiol Rev* **88**:125–172.

Garibaldi RA, Drusin RE, Ferebee SH, and Gregg MB (1972) Isoniazid-associated hepatitis. Report of an outbreak. *Am Rev Respir Dis* **106**:357–365.

Imai S and Guarente L (2014) NAD⁺ and sirtuins in aging and disease. *Trends Cell Biol* **24**: 464–471.

Kontani K, Nishina H, Ohoka Y, Takahashi K, and Katada T (1993) NAD glycohydrolase specifically induced by retinoic acid in human leukemic HL-60 cells. Identification of the NAD glycohydrolase as leukocyte cell surface antigen CD38. *J Biol Chem* **268**:16895–16898.

Lee HC (2012) Cyclic ADP-ribose and nicotinic acid adenine dinucleotide phosphate (NAADP) as messengers for calcium mobilization. *J Biol Chem* **287**:31633–31640.

Li F, Miao Y, Zhang L, Neuenswander SA, Douglas JT, and Ma X (2011) Metabolomic analysis reveals novel isoniazid metabolites and hydrazones in human urine. *Drug Metab Pharmacokinet* **26**:569–576.

Li F, Wang P, Liu K, Tarrago MG, Lu J, Chini EN, and Ma X (2016) A high dose of isoniazid disturbs endobiotic homeostasis in mouse liver. *Drug Metab Dispos* **44**:1742–1751.

Liu K, Zhu J, Huang Y, Li C, Lu J, Sachar M, Li S, and Ma X (2017) Metabolism of KO143, an ABCG2 inhibitor. *Drug Metab Pharmacokinet* **32**:193–200.

Malavasi F, Deaglio S, Funaro A, Ferrero E, Horenstein AL, Ortolan E, Vaisitti T, and Aydin S (2008) Evolution and function of the ADP ribosyl cyclase/CD38 gene family in physiology and pathology. *Physiol Rev* **88**:841–886.

March S, Graupera M, Rosa Sarrias M, Lozano F, Pizcueta P, Bosch J, and Engel P (2007) Identification and functional characterization of the hepatic stellate cell CD38 cell surface molecule. *Am J Pathol* **170**:176–187.

Mederacke I, Dapito DH, Affò S, Uchinami H, and Schwabe RF (2015) High-yield and high-purity isolation of hepatic stellate cells from normal and fibrotic mouse livers. *Nat Protoc* **10**:305–315.

Nelson SD, Mitchell JR, Timbrell JA, Snodgrass WR, and Corcoran GB III (1976) Isoniazid and iproniazid: activation of metabolites to toxic intermediates in man and rat. *Science* **193**:901–903.

Nolan CM, Goldberg SV, and Buskin SE (1999) Hepatotoxicity associated with isoniazid preventive therapy: a 7-year survey from a public health tuberculosis clinic. *JAMA* **281**:1014–1018.

Oei SL, Griesenbeck J, Buchlow G, Jorcke D, Mayer-Kuckuk P, Wons T, and Ziegler M (1996) NAD⁺ analogs substituted in the purine base as substrates for poly(ADP-ribosyl) transferase. *FEBS Lett* **397**:17–21.

Oesch F and Steinberg P (1987) A comparative study of drug-metabolizing enzymes present in isolated rat liver parenchymal, Kupffer and endothelial cells. *Biochem Soc Trans* **15**:372–373.

Peters JH, Miller KS, and Brown P (1965) Studies on the metabolic basis for the genetically determined capacities for isoniazid inactivation in man. *J Pharmacol Exp Ther* **150**:298–304.

Piscaglia F, Knittel T, Kobold D, Barnikol-Watanabe S, Di Rocco P, and Ramadori G (1999) Cellular localization of hepatic cytochrome 1B1 expression and its regulation by aromatic hydrocarbons and inflammatory cytokines. *Biochem Pharmacol* **58**:157–165.

Roberts RA, Ganey PE, Ju C, Kamendulis LM, Rusyn I, and Klaunig JE (2007) Role of the Kupffer cell in mediating hepatic toxicity and carcinogenesis. *Toxicol Sci* **96**:2–15.

Sachar M, Li F, Liu K, Wang P, Lu J, and Ma X (2016) Chronic treatment with isoniazid causes protoporphyrin IX accumulation in mouse liver. *Chem Res Toxicol* **29**:1293–1297.

Sarich TC, Adams SP, Petricca G, and Wright JM (1999) Inhibition of isoniazid-induced hepatotoxicity in rabbits by pretreatment with an amidase inhibitor. *J Pharmacol Exp Ther* **289**: 695–702.

Sarich TC, Youssefi M, Zhou T, Adams SP, Wall RA, and Wright JM (1996) Role of hydrazine in the mechanism of isoniazid hepatotoxicity in rabbits. *Arch Toxicol* **70**:835–840.

Scharer L and Smith JP (1969) Serum transaminase elevations and other hepatic abnormalities in patients receiving isoniazid. *Ann Intern Med* **71**:1113–1120.

Si-Tayeb K, Lemaigre FP, and Duncan SA (2010) Organogenesis and development of the liver. *Dev Cell* **18**:175–189.

Smedsrød B and Pertoft H (1985) Preparation of pure hepatocytes and reticuloendothelial cells in high yield from a single rat liver by means of Percoll centrifugation and selective adherence. *J Leukoc Biol* **38**:213–230.

Stein LR and Imai S (2012) The dynamic regulation of NAD metabolism in mitochondria. *Trends Endocrinol Metab* **23**:420–428.

Sugamori KS, Wong S, Gaedigk A, Yu V, Abramovici H, Rozmahel R, and Grant DM (2003) Generation and functional characterization of arylamine N-acetyltransferase Nat1/Nat2 double-knockout mice. *Mol Pharmacol* **64**:170–179.

Timbrell JA, Mitchell JR, Snodgrass WR, and Nelson SD (1980) Isoniazid hepatoxicity: the relationship between covalent binding and metabolism in vivo. *J Pharmacol Exp Ther* **213**: 364–369.

Wang P, Pradhan K, Zhong XB, and Ma X (2016) Isoniazid metabolism and hepatotoxicity. *Acta Pharm Sin B* **6**:384–392.

Wang P, Shehu AI, Lu J, Joshi RH, Venkataramanan R, Sugamori KS, Grant DM, Zhong XB, and Ma X (2017) Deficiency of N-acetyltransferase increases the interactions of isoniazid with endobiotics in mouse liver. *Biochem Pharmacol* **145**:218–225.

Wiegand RG (1956) The formation of pyridoxal and pyridoxal 5-phosphate hydrazones1. *J Am Chem Soc* **78**:5307–5309.

World Health Organization (2018) *Global Tuberculosis Report 2018*, World Health Organization, Geneva, Switzerland.

Yue J, Peng RX, Yang J, Kong R, and Liu J (2004) CYP2E1 mediated isoniazid-induced hepatotoxicity in rats. *Acta Pharmacol Sin* **25**:699–704.

Zamboni V and Defranceschi A (1954) Identification of isonicotinoylhydrazones of pyruvic and α-ketoglutaric acid in rat urine after treatment with isonicotinic acid hydrazide (isoniazid). *Biochim Biophys Acta* **14**:430–432.

Zatman LJ, Kaplan NO, Colowick SP, and Ciotti MM (1954) The isolation and properties of the isonicotinic acid hydrazide analogue of diphosphopyridine nucleotide. *J Biol Chem* **209**: 467–484.

Zhong Z, Goto M, Hijioka T, Oide H, Kauffman FC, and Thurman RG (1994) Role of Kupffer cells in storage and metabolism of benzo(a)pyrene in the liver. *Drug Metab Dispos* **22**:680–687.

Zhu J, Wang P, Shehu AI, Lu J, Bi H, and Ma X (2018) Identification of novel pathways in idelalisib metabolism and bioactivation. *Chem Res Toxicol* **31**:548–555.

Address correspondence to: Dr. Xiaochao Ma, Department of Pharmaceutical Sciences, Center for Pharmacogenetics, School of Pharmacy, University of Pittsburgh, 309 Salk Pavilion, 335 Sutherland Dr., Pittsburgh, PA 15261. E-mail: mxiaocha@pitt.edu